UC Davis

UC Davis Previously Published Works

Title

Memory effect in magnetic nanowire arrays.

Permalink

https://escholarship.org/uc/item/5t58v3hz

Journal

Advanced materials (Deerfield Beach, Fla.), 23(11)

ISSN

1521-4095

Authors

Kou, Xiaoming
Fan, Xin
Dumas, Randy K
et al.

Publication Date

2011-03-18

Peer reviewed

eScholarship.org Powered by the California Digital Library
University of California

Memory Effect in Magnetic Nanowire Arrays

*Xiaoming Kou, Xin Fan, Randy K. Dumas, Qi Lu, Yaping Zhang, Hao Zhu, Xiaokai Zhang, Kai Liu, and John Q. Xiao**

Magnetic materials are widely used for information storage because of their large capacity and low cost.[1] Storage medium technologies have evolved from analog recording with magnetic tapes to high fidelity digital recording with magnetic hard disks. Nevertheless, both techniques use a magnetic medium consisting of magnetic particles, whose sizes have also evolved from micrometers in magnetic tapes to nanometers in modern hard disks. In analog recording, signals are converted into magnetic fields which change the magnetization of a group of magnetic particles (bit). The magnetization variations represent the stored information which can subsequently be read out. The magnetization, and therefore the stored information, could be changed by an external magnetic field and/or thermal effects. In digital recording, the bit magnetization can be aligned either left or right in parallel recording or up and down in perpendicular recording.[2] The information is stable as long as the medium is not subjected to a magnetic field higher than the coercivity, or a temperature higher than the superparamagnetic limit, of the constituent magnetic particles. In order to clearly distinguish one bit from another it is advantageous to minimize the dipolar interaction among magnetic particles, which is typically achieved by creating boundaries between particles. Since the magnetic dipolar interaction is particularly pronounced in a collection of magnetic entities, such as magnetic particles and nanowires, it is scientifically interesting to question whether such a degree of freedom can be exploited in order to create additional memory functions. To answer this question, one needs a magnetic system with a sizable and preferably controllable dipolar interaction. The magnetic nanowire array is an ideal system for this purpose.

Magnetic nanowire arrays embedded in an insulating Al_2O_3 matrix have been intensively studied.[3–12] When the magnetocrystalline anisotropy is negligible, the magnetization direction of the nanowires is preferably aligned along the length of the nanowire because of the shape anisotropy. When nanowires are very close to each other, dipolar interactions play a significant role in the magnetic behavior of the nanowire array, leading to rich physical phenomena and great application potentials.[7–12] Recently, it was demonstrated that the dipolar interaction among magnetic nanowires could provide zero field ferromagnetic resonance (FMR) tunability, which has potential applications in a variety of microwave devices. A double FMR feature caused by the dipolar interaction in a magnetic nanowire array was also predicted[13] and verified.[14–17] In this manuscript, we demonstrate how dipolar interactions can induce an analog memory effect in magnetic nanowire arrays. Through this effect, the magnetic nanowire array has the ability to 'memorize' the maximum magnetic field that the array has been exposed to. A novel, low cost, and robust electromagnetic pulse detecting method is proposed based on this memory effect.

Nanowire arrays of $Ni_{90}Fe_{10}$ and Ni were synthesized by electrodeposition into anodized alumina templates. The diameter, center-to-center interpore distance, and length of the nanowires are 35 nm, 60 nm, and 30 μm, respectively. **Figure 1**a shows the hysteresis loop, with a coercivity of 1080 Oe, of a $Ni_{90}Fe_{10}$ nanowire array with a magnetic field parallel to the wire (open squares). The loop with the field perpendicular to the wire is shown in the inset. Clearly, a well defined easy axis exists along the wire axis because of the dominant shape anisotropy.

The memory effect was demonstrated using a vibrating sample magnetometer. The $Ni_{90}Fe_{10}$ nanowire array was saturated along the wire prior to the measurement. The magnetic moment of the array was monitored as a series of magnetic field pulses were applied parallel to the nanowires. Figure 1b displays the series of magnetic pulses with different magnitudes and directions. The corresponding change of the magnetic moment is illustrated in Figure 1c. We find that the magnetic moment decreases monotonically as the magnitude of the negative pulses increases, while the moment remains the same after the positive pulses. This demonstrates that the maximum negative magnetic field can be recorded into the nanowire array. However, this is violated for the 800 and 900 Oe field pulses, and this discrepancy will be explained later. The result is also plotted in the magnetic moment verses applied field (M–H) graph, displayed in Figure 1d. Similar properties are also observed in Ni nanowire arrays.

This phenomenon is attributed to the dipolar interactions among the nanowires. Previously, using a theoretical model, two assumptions were proposed.[13] First, each nanowire is a single domain cylinder with a uniform magnetization pointing up or down parallel to the wire. The second assumption is that the number of nanowires with up magnetizations ($N\uparrow$) and down magnetizations ($N\downarrow$) is determined by the total magnetization $M(H)$, i.e. $(N\uparrow - N\downarrow)/(N\uparrow + N\downarrow) = M(H)/M_s$, where M_s is the saturation magnetization. According to these assumptions, the dipolar field among the nanowires can be written as[13]

X. Kou, Dr. X. Fan, Q. Lu, Y. Zhang Prof. J. Q. Xiao
Department of Physics and Astronomy
University of Delaware
Newark, DE, 19716, USA
E-mail: jqx@udel.edu
Dr. R. K. Dumas, Prof. K. Liu
Department of Physics
University of California
Davis, CA, 95616, USA
Dr. H. Zhu, Dr. X. Zhang
Spectrum Magnetics
LLC, 1210 First State Blvd, Wilmington, DE, 19804, USA

DOI: 10.1002/adma.201003749

© 2011 WILEY-VCH Verlag GmbH & Co. KGaA, Weinheim

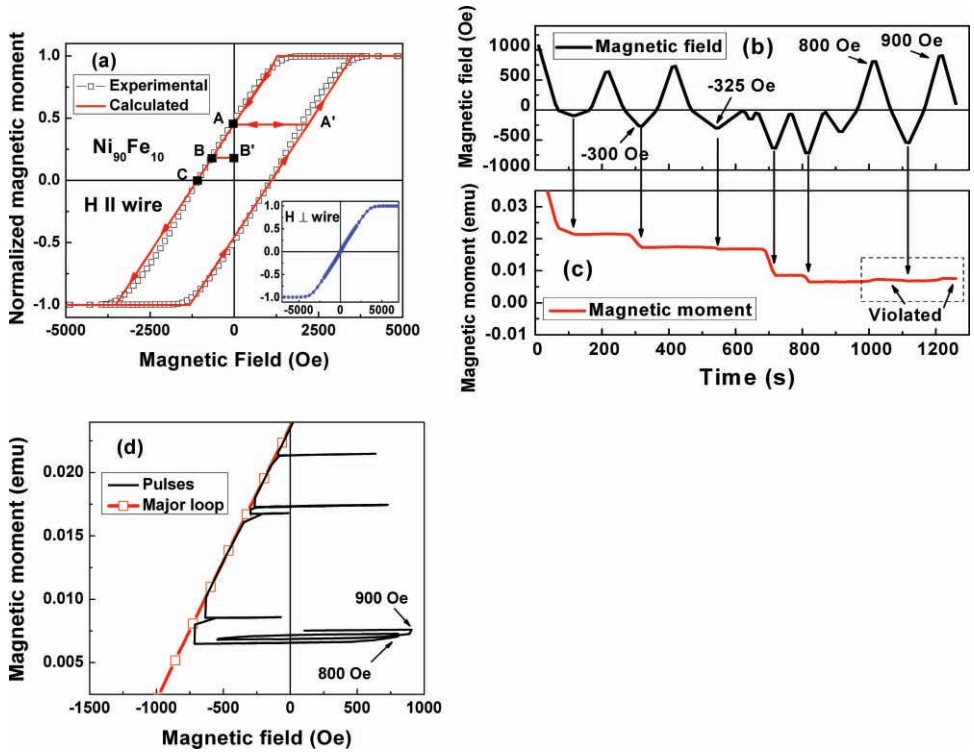

Figure 1. a) Measured (open square) and calculated (solid line) hysteresis loops of a $Ni_{90}Fe_{10}$ nanowire array with magnetic field along the wire. The change of the magnetization can only follow the direction of the arrows on the loop. When the field is removed at point B, the magnetization returns to B'. If a positive field smaller than $2H_c$ is applied at A, the magnetization moves between A and A' reversibly. The insert depicts the measured hysteresis loop with magnetic field perpendicular to the wires (solid circle). b) A series of magnetic pulses applied parallel to the $Ni_{90}Fe_{10}$ nanowires. c) The magnetic moment of the nanowire array was measured during the pulses. The negative pulses lower the magnetic remanent monotonically, while the positive ones do not change the moment except the 800 and 900 Oe pulses. The arrows are guides for the eyes. d) M-H plot of the magnetic moment changes under the pulses (solid line). The major loop is also included for comparison (open spare).

$$H_{\text{dipole}}(H) = -M(H) \times \beta \quad (1)$$

where H_{dipole} and H are the dipolar field among the nanowires and the applied field, respectively. β is a geometric factor, which depends only on the geometry of the nanowires including their diameter, length, and separation.

Based on this model, when the positive applied field is reduced from the saturation state, the first switching happens when $H_{\text{dipole}} + H$ exceeds the switching field of a single wire, H_{sw}. Subsequently, the magnetization $M(H)$ decreases by a small amount, and so does the dipole field H_{dipole}, according to Equation (1). The switching stops when $H_{\text{dipole}} + H$ is decreased below H_{sw}. A stable state is reached at the following condition

$$H_{\text{dipole}} + H = H_{\text{sw}} \quad (2)$$

The hysteresis loop can be reconstructed from Equation (2) after substituting the H_{sw} by the coercivity H_c, shown in Figure 1a (solid line). It can be inferred from this argument that the magnetic moment of the nanowire array remains unchanged as long as

$$|H_{\text{dipole}} + H| \leq H_{\text{sw}} \quad (3)$$

is satisfied. Hence, the change of the magnetization on the hysteresis loop is irreversible at descending field directions below the saturation field, as indicated with arrows in Figure 1a. For example, if the sample is at state A, the magnetization will change to B in a negative field and return to state B' once the field is removed. On the other hand, if the sample is at state A and subject to a positive field (along the AA' line), the sample will return to state A upon removal of the field reversibly as long as Equation (3) is satisfied. Therefore, a memory effect exists in the magnetic nanowire array as there is a one-to-one correspondence between the remanent and the negative field the sample was exposed to, as shown in Figure 1a. In other words the sample memorizes the maximum negative field in terms of remanent magnetization. The memory remains provided the magnitude of a positive field does not violate Equation (3). In using Equation (3), one typically uses the coercivity to represent the switching field. It should be emphasized that there is local variation in switching fields spread around the coercivity. Therefore, if the positive field pulse is close to the coercivity, one must be careful in using Equation (3). For example, as illustrated in Figures 1b and c, the magnetic moment increases slightly after the 800 and 900 Oe positive pulses. The dipolar field in this case is antiparallel to the positive pulses, therefore $|H_{\text{dipole}} + H|$ is smaller than H_c = 1080 Oe, and the magnetic moment should stay unchanged, contradictory to the experimental observation. Such a discrepancy is attributable to the distribution of the switching fields.

To further probe the interactions, switching field, and switching field distribution of the nanowires, first-order reversal curve (FORC)[18–22] measurements are performed on

© 2011 WILEY-VCH Verlag GmbH & Co. KGaA, Weinheim

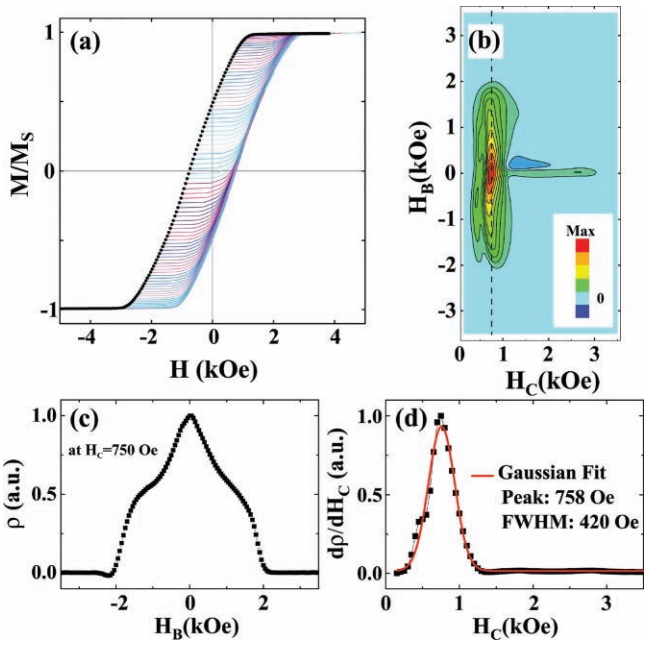

Figure 2. a) A family of FORCs for the Ni nanowire array with the applied field parallel to the wires. The black dots represent the starting point of each FORC. b) The corresponding FORC distribution plotted in (H_C, H_B) coordinates. The vertical black dashed line indicates the vertical line scan shown in (c) at H_C = 750 Oe. d) Projection of the FORC distribution onto the H_C-axis and Gaussian fit highlighting the mean switching field and its distribution.

a Ni nanowire array. FORC measurements proceed as follows: After positive saturation the applied field is reduced to a given reversal field, H_R. From this reversal field the magnetization is then measured back towards positive saturation, thereby tracing out a single FORC. This process is repeated for a series of decreasing reversal fields thus filling the interior of the major hysteresis loop. As shown in **Figure 2**a, under increasing applied magnetic fields, each of the FORCs traverses horizontally before conforming onto the major loop; the stacking of the FORCs leads to the one-to-one correspondence between the reversal field and the remanent magnetization.

The FORC distribution is then defined as a mixed second order derivative of the normalized magnetization:

$$\rho(H, H_R) \equiv -\frac{1}{2}\frac{\partial^2 M(H, H_R)/M_S}{\partial H \partial H_R}. \quad (4)$$

For our purposes here the FORC distribution is plotted in (H_C, H_B) coordinates, where H_C is the local coercive field and H_B is the local interaction or bias field. The transformation from (H, H_R) coordinates is accomplished by a simple rotation of the coordinate system defined by: $H_B = (H + H_R)/2$ and $H_C = (H - H_R)/2$. The FORC distribution of the Ni nanowire array shown in Figure 2b is dominated by a broad vertical ridge that runs parallel to the H_B-axis and indicates the presence of strong demagnetizing dipolar interactions.[19,21,22] A line scan, indicated in Figure 2b with a vertical dashed line, through this ridge is shown in Figure 2c. The ridge begins to deviate from zero at H_B ~ 2000 Oe, which indicates the maximum dipolar field, consistent with a calculated value of 1830 Oe from Equation (1). Furthermore, the FORC analysis allows the switching behavior to be separated from the dipolar broadening. We find that the vertical ridge is centered at H_C ~ 750 Oe, the coercivity of the major loop. Quantitative analysis of the switching behavior is best illustrated by integrating horizontal line scans, known as a projection along the H_C-axis $d\rho/dH_C$, as shown in Figure 2d (solid squares). A Gaussian fit of this FORC projection shows a peak at 758 Oe, with a full width at half maximum (FWHM) of 420 Oe. The peak location indicates the mean switching field while the FWHM is a direct quantitative measure of the distribution of switching fields among the ~10^9 nanowires measured. As there are finite fractions of nanowires with switching fields less than 750 Oe, the H_{sw} in Equation (3) is no longer a single value, but a distribution. Thus deviations from Equation (3) occur first in those wires. This can be clearly seen in the family of FORC curves in Figure 2a as the individual FORCs begin to turn upward before reaching the ascending-field branch of the major loop. The switching field distribution, which may be attributable to small variations in wire length, diameter, etc., ultimately limits the working range of the envisioned magnetic field pulse sensor.

Based on the memory effect, we propose an electromagnetic pulse (EMP) detection method. An EMP generated by a nuclear or non-nuclear explosion poses a threat to electronic and electrical devices by inducing a large current or voltage surge.[23] The detection of EMP is a challenging task because the detection system must be able to handle high peak field strengths. An optical method, based on measuring the polarization change induced by an EMP, might be one of the few operable methods that can survive.[24] However, the optical system is usually expensive and bulky. Magnetic nanowire arrays are robust to an EMP since they record magnetic pulses passively. Once the magnetic component is recorded and read out, the electric component of an EMP can be readily calculated from the impedance of the propagating media. In the following, the procedure of using a magnetic nanowire array to measure the magnetic field component of an EMP is described. The working scheme is illustrated in **Figure 3**.

1. Before each measurement, the nanowire array needs to be initialized to the state with the maximum remanent magnetization. This is achieved by saturating the nanowire array with a large positive magnetic field (Figure 3a) and subsequently removing the field (Figure 3b).
2. For simplicity, the magnetic field pulses are assumed to be always along the direction of the nanowires. In cases of pulses in other directions, more pieces of nanowire arrays can be combined together. When a series of magnetic pulses or EMP is present, the nanowire array records the strongest negative pulse, Figure 3c.
3. The nanowire array with a non-zero magnetization, behaves as a small permanent magnet. A localized magnetic field of a few Oe exists at the surface of the nanowire array and increases monotonically with the remanent moment of the nanowire array. This field can be easily detected with a magnetic field sensor (Figure 3d). For example, the surface field of a 5 mm × 5 mm $Ni_{90}Fe_{10}$ nanowire array is about 10 Oe in the maximum remanent state, as measured by a gaussmeter. After the surface field is read, the array is ready to be initialized for another measurement (Figure 3e).

© 2011 WILEY-VCH Verlag GmbH & Co. KGaA, Weinheim

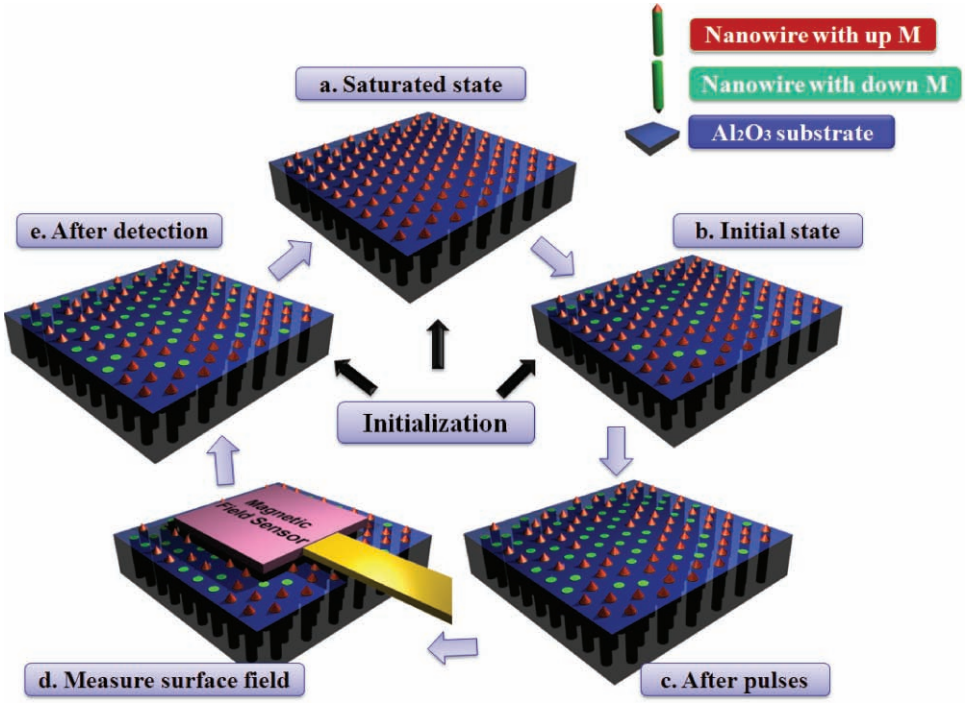

Figure 3. A novel magnetic field pulse detection scheme. a) Saturated by applying a strong positive field. b) Maximum remanent state after removing the field. c) The strongest negative pulse is recorded. d) Reading the surface field with a magnetic field sensor to find the remanent moment. e) Ready for another measurement cycle.

In summary, an analog memory effect in magnetic nanowire arrays has been demonstrated for the first time. The maximum magnetic field in a series of magnetic field pulses can be 'memorized' in the array. The origin of the memory effect is the dipolar interaction among nanowires, which is modeled with two basic assumptions. The deviation between the experimental result and the theory is clarified by measuring the switching field distribution among nanowires with the FORC technique. Based on the memory effect, a novel EMP detection scheme is proposed. Besides the extremely low cost, an EMP detector built with a magnetic nanowire array has the ability to measure a magnetic field component as high as a few hundred Oe without breaking down.

Experimental Section

Magnetic nanowire arrays were synthesized by electrodepositing magnetic metals into anodized alumina templates (AAT). The fabrication processes of the AAT and $Ni_{90}Fe_{10}$ nanowires are described elsewhere.[13] The diameter, interpore distance, and the length of the nanowires are 35 nm, 60 nm, and 30 μm, respectively. Ni nanowires of similar size were also fabricated by the same method. The bath for the Ni nanowires consisted of $NiSO_4 \cdot 6H_2O$ (120 g L^{-1}) and H_3BO_3 (45 g L^{-1}). Hysteresis loops were recorded by a vibrating sample magnetometer (Lakeshore 7404). FORCs were measured using a Princeton Measurements Corp. 2900 vibrating sample magnetometer. The size and composition of $Ni_{90}Fe_{10}$ and Ni nanowire arrays were determined by scanning electron microscopy and energy dispersive X-ray spectroscopy (JEOL JSM6335F). The surface field of the magnetic nanowire array was measured by a gaussmeter (Lakeshore 450).

Acknowledgements

This work has been supported by NSF DMR0827249 and NSF IIP-1013468. Work at UCD was supported by NSF DMR-1008791 and NSF ECCS-0925626.

Received: October 12, 2010
Revised: December 13, 2010
Published online: February 7, 2011

[1] R. C. O'Handley, *Modern Magnetic Materials Principles and Applications*, Wiley, New York **1999**.
[2] C. A. Ross, *Annu. Rev. Mater. Res.* **2001**, *31*, 203.
[3] L. Sun, Y. Hao, C. L. Chien, P. C. Searson, *IBM J. Res. Dev.* **2005**, *49*, 79.
[4] M. Darques, J. Spiegel, J. D. Medina, I Huynen, L. Piraux, *J. Magn. Magn. Mater.* **2009**, *321*, 2055.
[5] A. Fert, L. Piraux, *J. Magn. Magn. Mater.* **1999**, *200*, 338.
[6] X. F. Han, S. Shamaila, R. Sharif, J. Y. Chen, H. R. Liu, D. P. Liu, *Adv. Mater.* **2009**, *21*, 4619.
[7] A. Encinas, M. Demand, L. Piraux, I. Huynen, U. Ebels, *Phys. Rev. B* **2001**, *63*, 104 415.
[8] J. Escrig, D. Altbir, M. Jaafar, D. Navas, A. Asenjo, M. Vazquez, *Phys. Rev. B* **2007**, *75*, 184 429.
[9] M. Pardavi-Horvath, P. E. Si, M. Vazquez, W. O. Rosa, G. Badini, *J. Appl. Phys.* **2008**, *103*, 07D517.
[10] B. K. Kuanr, V. Veerakumar, R. Marson, S. R. Mishra, R. E. Camley, Z. Celinski, *Appl. Phys. Lett.* **2009**, *94*, 112 509.
[11] D. Serantes, D. Baldomir, M. Pereiro, B. Hernando, V. M. Prida, J. L. Sanchez Llamazares, A. Zhukov, M. Ilyn, J. Gonzalez, *J. Phys. D: Appl. Phys.* **2009**, 42.

© 2011 WILEY-VCH Verlag GmbH & Co. KGaA, Weinheim

[12] D.-L. Sun, J.-H. Gao, X.-Q. Zhang, Q.-F. Zhan, W. He, Y. Sun, Z.-H Cheng, *J. Magn. Magn. Mater.* **2009**, *321*, 2737.
[13] X. Kou, X. Fan, H. Zhu, J. Q. Xiao, *Appl. Phys. Lett.* **2009**, *94*, 112 509.
[14] L. P. Carignan, V. Boucher, T. Kodera, C. Caloz, A. Yelon, D. Menard, *Appl. Phys. Lett.* **2009**, *95*, 062 504.
[15] V. Boucher, L. P. Carignan, T. Kodera, C. Caloz, A. Yelon, D. Menard, *Phys. Rev. B* **2009**, *80*, 224 402.
[16] J. D. Medina, L. Piraux, A. Encinas, *Appl. Phys. Lett.* **2010**, *96*, 042 504.
[17] X. Kou, X. Fan, H. Zhu, R. Cao, J. Q. Xiao, *IEEE Trans. Magn.* **2010**, *46*, 1143.
[18] J. E. Davies, O. Hellwig, E. E. Fullerton, G. Denbeaux, J. B. Kortright, K. Liu, *Phys. Rev. B* **2004**, *70*, 224 434.
[19] C. R. Pike, C. A. Ross, R. T. Scalettar, G. T. Zimanyi, *Phys. Rev. B* **2005**, *71*, 134 407.
[20] R. K. Dumas, C. P. Li, I. V. Roshchin, I. K. Schuller K. Liu, *Phys. Rev. B* **2007**, *75*, 134 405.
[21] F. Beron, L.-P. Carignan, D. Menard, A. Yelon, *IEEE Trans. Magn.* **2008**, *44*, 2745.
[22] R. Lavin, J. C. Denardin, J. Escrig, D. Altbir, A. Cortes, H. Gomez, *IEEE Trans. Magn.* **2008**, *44*, 2808.
[23] J. S. Foster, E. Gjelde, W. R. Graham, R. J. Hermann, H. M. Kluepfel, R. L. Lawson, G. K. Soper, L. L. Wood, J. B. Woodard, "Report of the Commission to Assess the Threat to the Uni ted States from Electromagnetic Pulse (EMP) Attack", **2004** (http://www.empcommission.org, accessed January **2011)**.
[24] S. S. Sriram, S. A. Kingsley, J. T. Boyd, *US Patent 5 267 336*, **1993**.

© 2011 WILEY-VCH Verlag GmbH & Co. KGaA, Weinheim